

## Numerical Calculation and Experimental Research on Crack Arrest by Detour Effect and Joule Heating of High Pulsed Current in Remanufacturing

YU Jing<sup>1,\*</sup>, ZHANG Hongchao<sup>1</sup>, DENG Dewei<sup>2</sup>, HAO Shengzhi<sup>3</sup>, and IQBAL Asif<sup>4</sup>

*1 Institute of Sustainable Design and Manufacture, Dalian University of Technology, Dalian 116023, China*

*2 School of Materials Science and Engineering, Dalian University of Technology, Dalian 116023, China*

*3 Key Laboratory of Materials Modification by Laser, Ion and Electron Beams of Ministry of Education, Dalian University of Technology, Dalian 116023, China*

Received July 24, 2013; revised April 8, 2014; accepted April 14, 2014

**Abstract:** The remanufacturing blanks with cracks were considered as irreparable. With utilization of detour effect and Joule heating of pulsed current, a technique to arrest the crack in martensitic stainless steel FV520B is developed. According to finite element theory, the finite element(FE) model of the cracked rectangular specimen is established firstly. Then, based on electro-thermo-structure coupled theory, the distributions of current density, temperature field, and stress field are calculated for the instant of energizing. Furthermore, the simulation results are verified by some corresponding experiments performed on high pulsed current discharge device of type HCPD-I. Morphology and microstructure around the crack tip before and after electro pulsing treatment are observed by optical microscope(OM) and scanning electron microscope(SEM), and then the diameters of fusion zone and heat affected zone(HAZ) are measured in order to contrast with numerical calculation results. Element distribution, nano-indentation hardness and residual stress in the vicinity of the crack tip are surveyed by energy dispersive spectrometer(EDS), scanning probe microscopy(SPM) and X-ray stress gauge, respectively. The results show that the obvious partition and refined grain around the crack tip can be observed due to the violent temperature change. The contents of carbon and oxygen in fusion zone and HAZ are higher than those in matrix, and however the hardness around the crack tip decreases. Large residual compressive stress is induced in the vicinity of the crack tip and it has the same order of magnitude for measured results and numerical calculation results that is 100 MPa. The relational curves between discharge energies and diameters of the fusion zone and HAZ are obtained by experiments. The difference of diameter of fusion zone between measured and calculated results is less than 18.3%. Numerical calculation is very useful to define the experimental parameters. An effective method to prevent further extension of the crack is presented and can provide a reference for the compressor rotor blade remanufacturing.

**Keywords:** remanufacturing, crack arrest, numerical simulation, microstructure, high pulse current

### 1 Introduction

Global warming and other environmental concerns continue increasing as industrialization rapidly grows. Reducing energy consumption to preserve the environment is a critical issue. Remanufacturing could help to preserve the environment by reducing the resources and energy consumption during a product's life cycle.

Remanufacturing process of the retired products includes disassembly, cleaning, processing, assembly, running-in, etc., as shown in Fig. 1. To the remanufacturing blanks with remanufactureability(named after remanufacturing, it possesses the residual life which can complete a whole service cycle), advanced surface technology<sup>[1-2]</sup> is adopted

to recover the surface size and make the remanufacturing parts superior to the original ones, or the advanced manufacturing technique<sup>[3]</sup> is applied to process the parts to satisfy the assembly requirements. In past, the remanufacturing blanks with cracks were thought as irreparable. The core parts of large mechanical equipment (such as engineering machinery, ship, airplane, large-scale compressor) are costly, highly value-added, complexly processed and possess high technological requirements. Processing these parts with cracks is highly desired not only from economic considerations but also for their sustainable and reliable application.

Retarding or arresting the crack growth can be achieved by reducing crack tip stress intensity<sup>[4]</sup>, introducing residual compressive stress<sup>[5]</sup>, and reducing crack tip stress concentrations<sup>[6]</sup>. Stop-hole drilling at the crack tip or in the direction of the crack propagation is commonly used in practice. Yet new fatigue cracks can initiate at the edge of the stop-hole, thus, the effectiveness of crack arrest

\* Corresponding author. E-mail: yj.0730.kb@163.com

Supported by National Basic Research Program of China(973 Program, Grant No. 2011CB013402)

© Chinese Mechanical Engineering Society and Springer-Verlag Berlin Heidelberg 2014

depends on the size of stop-hole and machining precision. Moreover, it is especially difficult to drill on highly hard

and brittle materials; it is only suitable for surface cracks, not applicable to internal defects or embedded cracks.

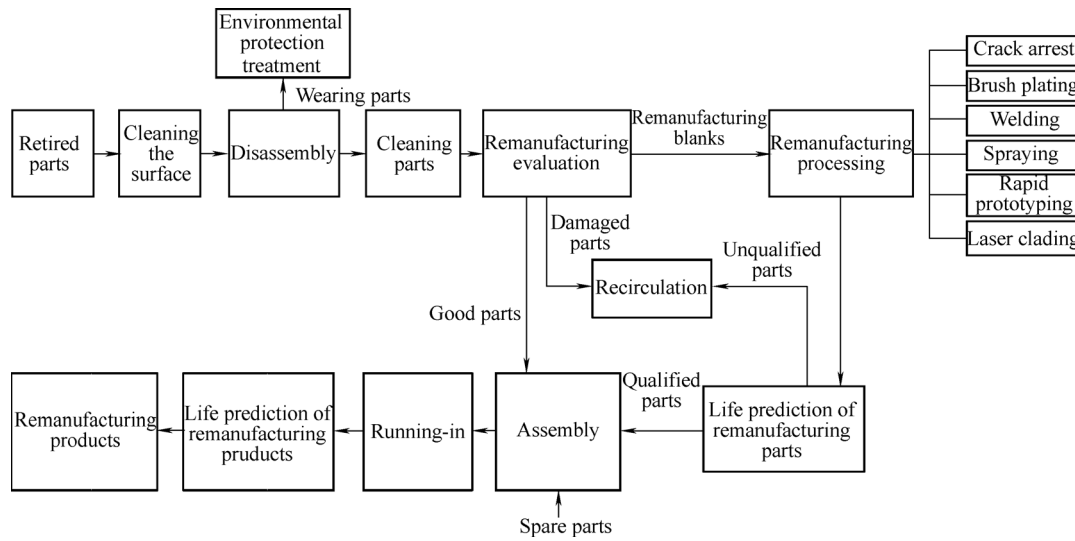


Fig. 1. General flow chart of a remanufacturing process

During recent years, the high density electro pulsing treatment of materials has attracted more and more attention due to its unique characteristics, and it is widely applied as a very promising non-equilibrium processing technology for practical solution, such as the modification of materials<sup>[7]</sup>, refining solidification structure<sup>[8]</sup>, improving the fatigue performance of metals<sup>[9]</sup>, and healing damage<sup>[10]</sup>.

It is known that when pulsed current flows through a conductive metal containing a crack or defect, the current will detour and concentrate at the crack tip. Due to Joule heating release, the local temperature increases that initiates crack tip melting, a round molten hole may occur at the crack tip and local thermal compressive stress can be induced. These phenomena cause prevention of crack growth and at the same time increases potential energy of formation of the main crack.

The effects of electromagnetic fields produced by current pulses on the kinetics of crack growth were examined in the work of GOLOVIN, et al<sup>[11]</sup>. The authors found out that when the current pulses were passed at appropriate time, the crack growth was prevented. The temperature field and stress field of the specimens containing two-dimensional<sup>[12-13]</sup> cracks and three-dimensional<sup>[14-15]</sup> cracks were derived by the methods of integral transformation and complex variable functions. FU, et al<sup>[16-17]</sup>, investigated the pulsed current discharge experiments and mechanical tests on embedded crack and welded joints. The phase change zone and microstructure near the crack tip were analyzed after performing electro pulsing treatment by WANG, et al<sup>[18]</sup> and GAO, et al<sup>[19]</sup>. The results showed that the local refined microstructure and residual stress near the crack tip had a long term effect for preventing crack growth. According to LIU<sup>[20-22]</sup>, the process of crack arrest by Joule heating was solved by using the finite element method based on thermo-electro-structural coupled theory. The remote tensile stress,

the temperature-dependent characteristic parameters and phase change were considered in the work. CAI, et al<sup>[23-24]</sup>, calculated the stress generated by detour effect and Joule heating that in turn were caused by the pulsed current in a numerical analysis procedure. The result showed that the thermal stress was beneficial for controlling the damage propagation.

This method provides a new way to retard crack growth. Local electric current and heat concentration only affect the crack tip. The nondefected portion of the remanufacturing blank remains unchanged. Moreover, it is not necessary to detect the location, size, or shape of the crack. We have a strong interest to investigate these effects of pulsed current on the crack arrest in remanufacturing.

The material FV520B, used in the manufacture of compressor rotor blade, is put under investigation in this paper. Based on thermo-electro-structural coupled field theory, the current density, temperature field, and stress field around the crack tip are calculated with the help of a finite element analysis software. The isotherm around the crack tip is used to estimate the size of fusion zone. The crack arrest experiments are performed on a self-designed high pulsed current discharge device of type HCPD-I. The macro/microstructures, element distribution, nano-indentation hardness and residual stress after electro pulsing treatment are investigated to explore the crack arrest effect of pulsed current and physical mechanisms. The sizes of the fusion zone and HAZ under various discharge energies are quantified. Afterwards, comparisons between experimental and simulated results are presented.

## 2 Numerical Calculation and Analysis

### 2.1 Problem statement

The material investigated is high strength martensitic stainless steel FV520B. In this paper, the main purpose is to

study the detour effect and Joule heating concentration at the crack tip. The heat is produced by electromagnetic field, which in turn, is produced by pulsed current. In this regard, the slit can substitute for a crack. The dimension of the specimen is shown in Fig. 2. A unilateral slit is prepared by wire-electrode cutting on the center of the longer side that penetrates throughout the thickness. The electric energy is applied on both the shorter sides. The temperature-dependent material properties are presented in Table 1, while Poisson's ratio of the material is 0.295, and density is  $7780 \text{ kg/m}^3$ .

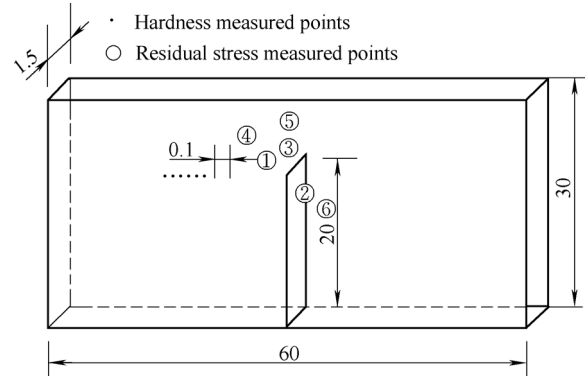


Fig. 2. Dimension of specimen / mm

Table 1. Temperature-dependent material properties

Temperature $t / ^\circ\text{C}$	Young's modules $E / \text{GPa}$	Coefficient of thermal expansion $\alpha / (^\circ\text{C})^{-1}$	Thermal conductivity $k / (\text{W} \cdot \text{m}^{-1} \cdot (^\circ\text{C})^{-1})$	Specific heat $c / (\text{J} \cdot \text{kg}^{-1} \cdot (^\circ\text{C})^{-1})$	Resistivity $\rho / (\Omega \cdot \mu\text{m})$
20	191	$10.80 \times 10^{-6}$	44.06	460	0.124 4
100	185	$10.53 \times 10^{-6}$	42.51	474	0.164 8
200	181	$10.16 \times 10^{-6}$	37.42	511	0.287 6
300	168	$11.36 \times 10^{-6}$	33.87	563	0.395 7
400	127	$12.24 \times 10^{-6}$	30.97	621	0.503 4
500	54	$12.96 \times 10^{-6}$	29.17	676	0.674 4
600	7.8	$13.50 \times 10^{-6}$	28.86	758	0.817 8
700	6.9	$14.58 \times 10^{-6}$	27.64	1005.4	1.100 9
800	—	$13.05 \times 10^{-6}$	23.73	1005.4	1.117 5
900	—	—	20.26	1005.4	1.182 0
1000	—	—	17.25	1298.7	1.254 0
1200	—	—	17.25	1298.7	1.376 0

## 2.2 Theories of analysis

Based on thermo-electro-structural coupled method, the temperature and stress fields in the vicinity of the crack tip are calculated when pulsed current is passed through the specimen. In the thermal analysis, nonlinear transient temperature field is derived. In the stress analysis, stress field is worked out.

The governing equations of the electrical analysis are as follows<sup>[25]</sup>:

$$\mathbf{E} = -\nabla\phi, \mathbf{J} = \frac{1}{\rho}\mathbf{E}, \nabla \cdot \mathbf{J} = 0, \quad (1)$$

where  $\mathbf{E}$ —Electric field,

$\mathbf{J}$ —Electric current density in the conductor,

$\phi$ —Electric potential,

$\rho$ —Resistivity of the metal conductor.

The temperature field around the crack tip can be obtained from the following relations<sup>[25-26]</sup>:

$$\dot{\mathbf{q}} = -k\nabla T, k\nabla T + \dot{\mathbf{q}} = \beta C_p \frac{\partial T}{\partial t}, \dot{\mathbf{q}} = \rho |\mathbf{J}|^2, \quad (2)$$

where  $\dot{\mathbf{q}}$ —Heat flux,

$k$ —Thermal conductivity of the metal conductor,

$T$ —Temperature field distribution of the conductor,

$\dot{\mathbf{q}}$ —Heat generation of Joule heat,

$\beta$ —Mass density of the metal conductor,

$C_p$ —Specific heat of the metal conductor,

$t$ —Conduction time.

The stress field in the vicinity of the crack tip can be calculated from the thermoelastic equations<sup>[27]</sup>:

$$\sigma_{ji,j} + X_i = \beta \ddot{u}_i, \quad (3)$$

$$\varepsilon_{ij} = \frac{1}{2}(u_{i,j} + u_{j,i}), \quad (4)$$

$$\varepsilon_{ij} = \frac{1}{E}[(1+\nu)\sigma_{ij} - (\nu I_1 - E\alpha\Delta T)\delta_{ij}], \quad i, j = x, y, z, \quad (5)$$

where  $\sigma_{ij}$ —Stress induced by electro pulsing,

$\varepsilon_{ij}$ —Volumetric strain,

$X_i$ —Body force,

$u_i$ —Displacement induced by temperature in the conductor,

$\ddot{u}_i$ —Acceleration,

$E$ —Young's modulus of the metal conductor,

$\alpha$ —Linear expansivity of the metal conductor,

$\nu$ —Poisson's ratio of the metal conductor,

$I_1$ —Stress invariant,

$I_1 = \sigma_{xx} + \sigma_{yy} + \sigma_{zz}$ ,

$\Delta T$  —Temperature difference,  
 $\Delta T = T - T_0$ ,  $T_0$  is the reference temperature,  
 $\delta_{ij}$  —Kronecker delta.

The finite element equation of the coupled field analysis is listed as follows<sup>[28]</sup>:

$$\begin{pmatrix} \mathbf{M} & \mathbf{0} & \mathbf{0} \\ \mathbf{0} & \mathbf{0} & \mathbf{0} \\ \mathbf{0} & \mathbf{0} & \mathbf{0} \end{pmatrix} \begin{pmatrix} \ddot{\mathbf{U}} \\ \ddot{\mathbf{T}} \\ \ddot{\mathbf{V}} \end{pmatrix} + \begin{pmatrix} \mathbf{C} & \mathbf{0} & \mathbf{0} \\ \mathbf{C}^{tu} & \mathbf{C}^t & \mathbf{0} \\ \mathbf{0} & \mathbf{0} & \mathbf{0} \end{pmatrix} \begin{pmatrix} \dot{\mathbf{U}} \\ \dot{\mathbf{T}} \\ \dot{\mathbf{V}} \end{pmatrix} + \begin{pmatrix} \mathbf{K} & \mathbf{K}^{ut} & \mathbf{0} \\ \mathbf{0} & \mathbf{K}^t & \mathbf{0} \\ \mathbf{0} & \mathbf{0} & \mathbf{K}^v \end{pmatrix} \begin{pmatrix} \mathbf{U} \\ \mathbf{T} \\ \mathbf{V} \end{pmatrix} = \begin{pmatrix} \mathbf{F} \\ \mathbf{Q} \\ \mathbf{I} \end{pmatrix}, \quad (6)$$

where  $\mathbf{U}$ ,  $\mathbf{T}$ ,  $\mathbf{V}$ ,  $\mathbf{F}$ ,  $\mathbf{Q}$  and  $\mathbf{I}$  are the vector forms of the displacement, temperature, electric potential, force, heat flow rate and electric current, respectively. The material constant matrices  $\mathbf{M}$ ,  $\mathbf{C}$ ,  $\mathbf{C}^{tu}$ ,  $\mathbf{C}^t$ ,  $\mathbf{K}$ ,  $\mathbf{K}^{ut}$ ,  $\mathbf{K}^t$ , and  $\mathbf{K}^v$  are the structural mass, structural damping, thermoelastic damping, specific heat, structural stiffness, thermoelastic stiffness, thermal conductivity and electric conductivity, respectively.

### 2.3 Numerical calculation results and analysis

The dimension of specimen, used in this section, is plotted in Fig. 2. Five kilojoules electric energy was applied on both shorter sides. The distribution of the electric current density, temperature field, and stress field at the crack tip were calculated. Fig. 3 shows that due to the existence of the crack, the current cannot pass through the crack surfaces and thus, the electric current detours and concentrates around the crack tip. This process results in the generation of large amount of Joule heating, and consequently, the temperature becomes higher than the fusion point, as shown in Fig. 4. From the numerical simulation, the average diameter of the circle-like fusion zone is about 0.824 mm. Fig. 5 shows that at the energizing moment, the annular compressive stress field is formed in the vicinity of the crack tip, which proves to be good for stopping the crack growth<sup>[18]</sup>. The detour effect and Joule heating affect only the area of the crack tip, so the other parts of the remanufacturing blank remain unaffected. Therefore, this method is especially suitable for large-sized remanufacturing blanks.

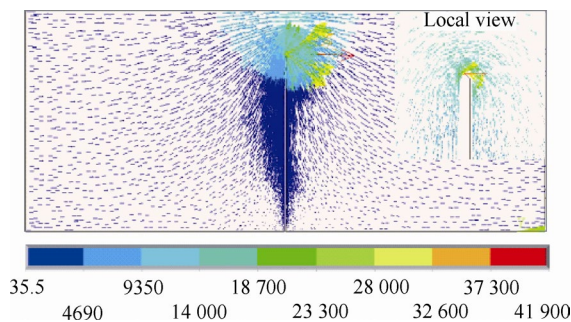


Fig. 3. Electric current density vectors  $J / (\text{A} \cdot \text{mm}^{-2})$

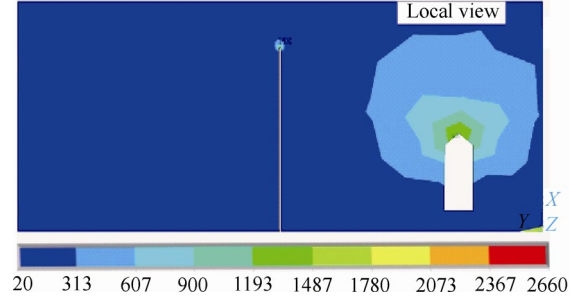


Fig. 4. Temperature field  $T / ^\circ\text{C}$

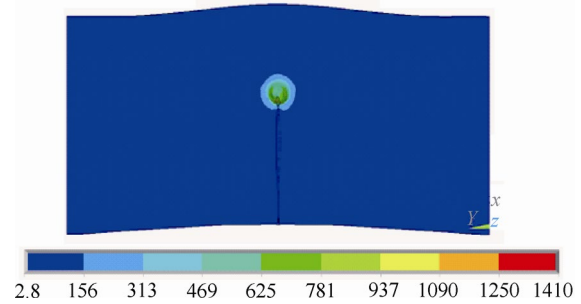


Fig. 5. Von mises stress field  $\sigma / \text{MPa}$

## 3 Experiments

The crack arrest experiments were performed under ambient conditions on a self-designed high pulsed current discharge device of type HCPD-I, as shown in Fig. 6(a). Fig. 6(b) shows the circuit diagram of the electro pulsing equipment. It is composed of an electric governor T, a high-tension transformer B, a rectifying silicon stack D, a current limiting resistor R, a tension switch S, capacitors C, and load. The basic parameters are as shown in Table 2.

Table 2. Parameters of electro pulsing equipment

Equipment parameter	Value
Energy storage of capacitors $C / \text{kJ}$	1–10
Discharge voltage $U / \text{kV}$	4–10
Peak current $I_{\text{PPM}} / \text{kA}$	250
Pulse duration $t_p / \mu\text{s}$	40–100

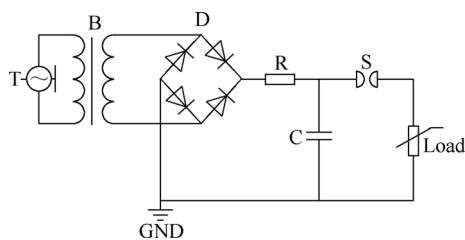
The pulse current was applied onto the specimen through two copper electrodes, as plotted in Fig. 6(c). In the discharge process, local fusion and eruption occurred at the crack tip because of detour effect and Joule heating accompanied by sparks and intense sound. As a result, a small hole is formed, and the crack tip becomes blunt. With increase of energy input, the current density and heat concentration ahead of the crack tip is larger, and the melting process gets more intense.

The geometry of specimens used is shown in Fig. 2. The samples were divided into two groups: the first one was not subjected to electro pulsing and was employed as reference; while the second one was treated under discharge energies 3 kJ, 4 kJ, and 5 kJ. Optical microscopy(OM) was employed

to measure diameters of the fusion zone and the HAZ. Afterwards, the specimens were made into metallographic samples to examine the morphology and microstructure around the crack tip after electro pulsing treatment by optical microscope(ML7000E-DG, China) as well as scanning electron microcopy(SEM, Evo18, Carl Zeiss Jsm-5310, Germany). The element distribution around the crack tip was determined using energy dispersive spectrometer(EDS). Nano-indentation hardness was measured by scanning probe microscopy(SPM, MTS Nano Indenter XP, USA). Residual stress around crack tip was evaluated using  $2\theta - \sin^2\psi$  technology on an X-ray stress gauge(X-350A, China). The measured points of hardness and residual stress measurements are exhibited in Fig. 2.



(a) Pulsed current discharge device



(b) Main circuit of discharge device



(c) Electrical discharge instant

Fig. 6. Experimental device and process

## 4 Experimental Results and Analysis

### 4.1 Morphology and microstructure around the crack tip

Fig. 7 shows the morphology and microstructure in the

vicinity of the crack tip after electro pulsing treatment. As shown in Fig. 7(a), after performing the crack arrest, the shape of the crack tip becomes obtuse and smooth. There are no serrated convexes or concaves; neither are there any secondary cracks. As the current cannot flow through the crack, the current has to detour around the crack tip, which causes the current density to increase excessively. Because of Joule heating, local melting occurs at the crack tip. The partition around the crack tip is distinct. As shown in Fig. 7(b), the microstructure of area A is very fine. It is actually the edge of the molten hole covered by fusion metal(white-bright layer). Fig. 7(c) shows area B located outside the white-bright layer. Color change is visible, which means that the local temperature is higher in this region. It does not reach the fusion point but does reach the phase change temperature. Area B is actually the heat affected zone(HAZ). The matrix microstructure in area C remains unchanged during electro pulsing treatment as shown in Fig. 7(d). The reason is that the effects of detour and Joule heating are weak over there, and thus, the temperature of matrix stays low. It is the characteristic that the nondefected part of component remains unchanged.

During the process of electro pulsing treatment, the rapid heating increases the nucleation rate. After the discharge process of pulse electric current, the growth of nucleated grains is restrained by the surrounding cool matrix. This, consequentially, results in the formation of fine cryptocrystalline martensite, and decentralization of the deformation, and reduction in stress concentration. It also suppresses the grain-boundary cracks and crack propagation so as to prolong the fatigue life<sup>[29]</sup>. The boundaries around areas A, B and C are clearly detectable, and they show a huge temperature gradient around the crack tip that would cause diversion of the crack propagation and prolonging the fatigue life of products<sup>[30]</sup>.

### 4.2 Element distribution around the crack tip

The element distribution around the crack tip is exhibited in Fig. 8. The contents of carbon and oxygen in the fusion zone and HAZ are higher than those in matrix. Due to electro pulsing treatment in atmosphere, the complex metallurgical, physical, and chemical process occurred between oxygen ions, produced by ionization, and fusion metal. It induced higher oxygen content. The higher content of carbon is regarded as that the passage of pulsed current through the specimen is followed by Joule heating release served as the activation energy for the initial carbide particles dispersively re-precipitated in the martensite matrix. When pulse current passes through the specimen, not only compressive stress is generated, but also a strong electronic wind is caused by a huge quantity of electrons. The electric current is much more sensitive to carbide than martensite, hence a mass of precipitated carbide concentrates at the crack tip.

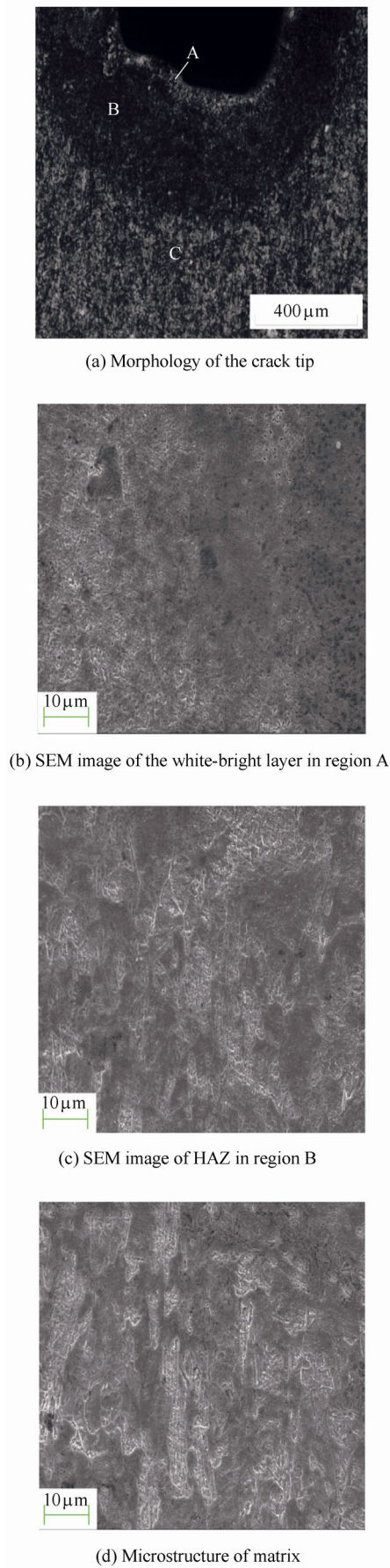


Fig. 7. OM/SEM images around crack tip after electro pulsing treatment

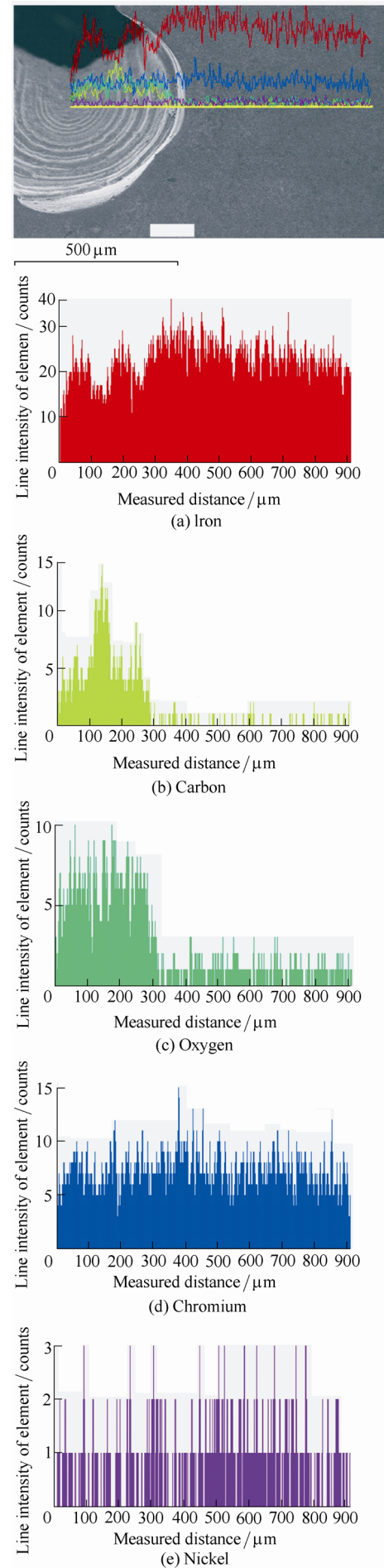


Fig. 8. Element distribution around the crack tip

### 4.3 Hardness measurements

Due to the very small sized white-bright layer, the first measured point was located in HAZ. As illustrated in Fig. 9, nano-indentation hardness beyond 0.3 mm is observed close to the matrix (5.755 GPa). Original precipitation hardening condition is altered due to the recrystallization effect and fine cryptocrystalline martensite is formed in the HAZ. The hardness decreases, but plasticity and toughness increase. It also shows the increase of crack initiation and propagation work<sup>[31]</sup> around the crack tip. Therefore, the crack growth becomes more difficult.

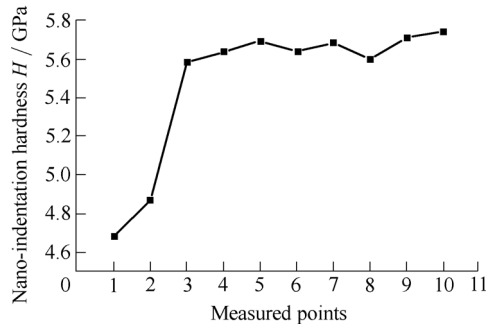


Fig. 9. Nano-indentation hardness around the crack tip

### 4.4 Residual stress measurements

Table 3 shows that large residual compressive stress is formed around the crack tip after electro pulsing treatment. At the instant of pulse current passing through the specimen, temperature around the crack tip increases sharply, and it initiates melting. On the other hand, the matrix remains almost at the room temperature. The expansion of the fusion zone and the HAZ with high temperature is restricted by the surrounding matrix which is at low temperature. Therefore, a huge compressive stresses,

which is superposition of phase transition stress and thermal stress, is formed around the crack tip. This is seen as a benefit to prevent crack growth and suppress generation of new micro-cracks. Stress intensity factor of the crack tip is reduced by large residual compressive stress<sup>[32]</sup>. It can create such a large inhibition effect on crack initiation and growth that is beneficial for improvement of the service lifetime of components. The compressive stress in the vicinity of the crack tip has the same order of magnitude for experimental data and calculated results, that is 100 MPa.

Table 3. Average value of residual stress




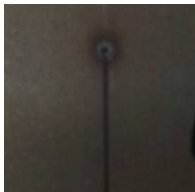
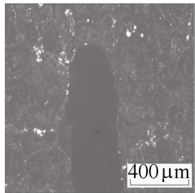
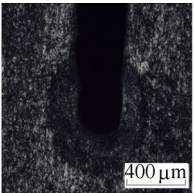
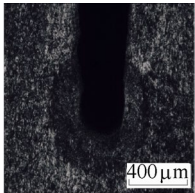
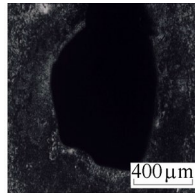
Measured point	Residual stress $\sigma$ / MPa	Error $\Delta$ / MPa
①	-152.25	$\pm 33$
②	-152.00	$\pm 23$
③	-159.50	$\pm 40$
④	-205.15	$\pm 43$
⑤	-174.20	$\pm 35$
⑥	-200.30	$\pm 27$

### 4.5 Relationships between the discharge energy and changes of the crack tip

The input energies 3, 4, and 5 kJ were, respectively, fed to the three specimens. Three specimens were treated by the respective discharge energy, and the diameters of the molten holes and HAZ were measured. The attained data was worked upon to obtain the average value. The relationship between discharge energy and sizes of molten zone and HAZ is explained in this section.

Table 4 shows the morphology and the microstructure at the crack tip observed under an optical microscope, and measurements of the diameters of the fusion zone and the HAZ produced by current burning.

Table 4. Average diameter of fusion zone, HAZ, morphology and microstructure around the crack tip

Discharge energy $W$ / kJ	Non-discharge	3	4	5
Fusion zone diameter $d_f$ / mm	0.2	0.344	0.573	0.702
Calculated diameter $d_c$ / mm	0.2	0.408	0.634	0.824
HAZ diameter $d_H$ / mm	$\times$	0.839	1.071	1.298
Macro morphology of the crack tip				
Metallographic structure of the crack tip				

From Table 4, when discharge energy is 3 kJ, no melting occurs at the macroscopic level, and only a snuff colored HAZ circle is observed around the crack tip. However,

under the optical microscope, there is a little melting around the crack tip, and the average diameter of the crack tip expands from 0.2 to 0.344 mm. When the discharge

energy is 4 or 5 kJ, the obtuse crack tip and local fusion phenomenon can be observed directly. A circular hole is formed at the crack tip. The fusion metal is rapidly solidified, and a white-bright layer, covering the crack tip, is formed. The snuff colored HAZ surrounds the layer from the outside. The average diameters of the holes are, respectively, 0.537 and 0.702 mm for the discharge energy of 4 and 5 kJ. With increase in discharge energy, the melting process becomes more severe, and diameters of the molten hole and HAZ become larger. It can, thus, be safely stated that the curvature radius of the crack tip can be controlled by adjustments in the discharge energy. Furthermore, the stress concentration factor can be reduced and crack growth can be halted.

The relational curves between discharge energy and diameters of the fusion zone and HAZ are obtained by experiments and simulation as shown in Fig. 10. Larger sizes of fusion zone and HAZ are obtained when the discharge energy is larger; thus, they are in positive correlation. The average difference of diameters of fusion zone between measured and calculated results is less than 18.3 %.

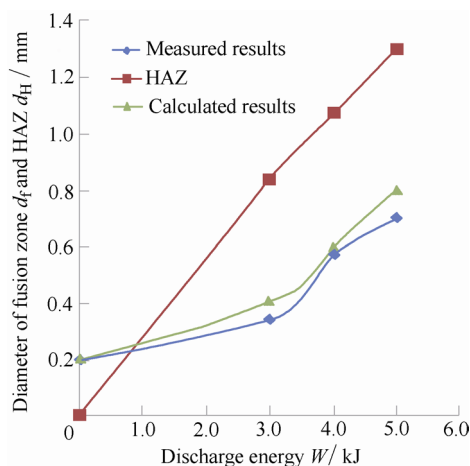


Fig. 10. Sizes of fusion zone and HAZ versus discharge energy

## 5 Conclusions

(1) Application of detour effect and Joule heating on arrest crack propagation is a kind of high efficiency and simple repair method for a remanufacturing blank. In the repair process, it affects only the area of crack tip, so that the other parts of the blank remain unaffected.

(2) The experimental results suggest that after electro pulsing treatment, the crack tip gets blunt, and the crack initiation is barricaded. The low hardness region with the high toughness and plasticity in HAZ would hinder the propagation of the crack. The large residual compressive stress around the crack tip is beneficial for suppressing crack initiation and propagation, and, for a long term, improving the service lifetime of components.

(3) The agreement between experimental and simulation results is very well. The difference of fusion zone between

numerical and experimental results is less than 18.3 %. The order of residual stress in experiment is same as that in numerical simulation. The results of simulation can provide reference for the experimental parameters selection. It is useful for the compressor rotor blade remanufacturing.

## References

- [1] LIU Zhengdao, ZHANG Xiancheng, XUAN Fuzhen, et al. Effect of laser power on the microstructure and mechanical properties of TiN/Ti3Al composite coating on Ti6Al4V[J]. *Chinese Journal of Mechanical Engineering*, 2013, 26(4): 714–721.
- [2] TAN Jun, CHEN Jianmin, LIU Min, et al. Surface engineering towards green manufacturing and remanufacturing[J]. *Journal of Mechanical Engineering*, 2011, 47(20): 95–103. (in Chinese)
- [3] XU Binshi, DONG Shiyun, ZHU Sheng, et al. Prospects and developing of remanufacture forming technology[J]. *Journal of Mechanical Engineering*, 2012, 48(15): 96–105. (in Chinese)
- [4] TU J F, PALEOCRASSAS A G. Fatigue crack fusion in thin-sheet aluminum alloys AA7075-T6 using low-speed fiber laser welding[J]. *Journal of Materials Processing Technology*, 2011, 211: 95–102. (in Chinese)
- [5] SCHNUBEL D, HORSTMANN M, VENTZKE V, et al. Retardation of fatigue crack growth in aircraft aluminium alloys via laser heating-Experimental proof of concept[J]. *Materials Science & Engineering A*, 2012, 546: 8–14.
- [6] SONG P S, SHIEH Y L. Stop drilling procedure for fatigue life improvement[J]. *International Journal of Fatigue*, 2004, 26: 1333–1339.
- [7] ZHAO Yuguang, MA Bingdong, GUO Haicha, et al. Electropulsing strengthened 2GPa boron steel with good ductility[J]. *Materials and Design*, 2013, 43: 195–199.
- [8] YIN Zhenxing, LIANG Dong, CHEN Yue, et al. Effect of electrodes and thermal insulators on grain refinement by electric current pulse[J]. *Transactions of Nonferrous Metals Society of China*, 2013, 23: 92–97.
- [9] LIU Yan, ZHOU Hong, SU Hang, et al. Effect of electrical pulse treatment on the thermal fatigue resistance of bionic compacted graphite cast iron processed in water[J]. *Materials and Design*, 2012, 39: 344–349.
- [10] ZHOU Y Z, GAO J D, GAO M. Crack healing in a steel by using electropulsing technique[J]. *Materials Letters*, 2004, 58: 1732–1736.
- [11] GOLOVIN Y I, FINKEL V M, SLETKOV A.A. Effects of current pulse on crack propagation kinetics in silicon iron[J]. *Problemy Prochnosti*, 1975 (2): 86–91.
- [12] FAN Hualin, CHEN Ping. Crack arrest effect in thin plates[J]. *Acta Arm Amentarii*, 2005, 26(6): 791–794. (in Chinese)
- [13] ZHANG Hongchao, YU jing, HAO Shengzhi, et al. Application of electro-magnetic heat effect on arresting the crack in remanufacturing blank[J]. *Journal of Mechanical Engineering*, 2013, 49(7): 21–28. (in Chinese)
- [14] FU Yuming, TIAN Zhengguo, ZHENG Lijuan. Analysis on the thermal stress field when crack arrest in an axial symmetry metal die using electromagnetic heating[J]. *Applied of Mathematics and Mechanics*, 2006, 8(3): 53–55.
- [15] ZHENG Lijuan, FU Yuming, TIAN Zhengguo, et al. Analysis on temperature field on a metal component with a circle half-embedding crack at the moment when the current is switched on[J]. *Journal of Mechanical Engineering*, 2004, 40(11): 90–93. (in Chinese)
- [16] FU Yuming, ZHOU Hongmei, WANG Junli, et al. Analysis of crack arrest by electromagnetic heating in metal with oblique-elliptical embedding crack[J]. *Key Engineering Materials, Advances in Fracture and Damage Mechanics XI*, 2012, 525–526: 404–408.
- [17] FU Yuming, CHAI Xuan, ZHENG Lijuan, et al. Pulse discharge



- strengthening of 16Mn welded joint and mechanical performance[J]. *Advanced Materials Research, Advanced Materials Research*, 2011, 197–198: 1460–1463.
- [18] WANG Ping, BAI Xiangzhong. Phase transformation stress and its influence for arresting crack propagation using electro-heating effect[J]. *China Mechanical Engineering*, 2011, 22(8): 980–984. (in Chinese)
- [19] GAO Diankui, LI Hui, FU Yuming, et al. Acted a pulse current to prevent the thermal fatigue crack subcritical extending[J]. *Journal of Mechanical Engineering*, 2001, 37(11): 28–31. (in Chinese)
- [20] LIU T J C. Thermo-electro-structural coupled analyses of crack arrest by Joule heating[J]. *Theoretical and Applied Fracture Mechanics*, 2008, 49: 171–184.
- [21] LIU T J C. Application of Thermo-Electric Joule Heating for Crack Detection[C]//*International Conference on Mechanical and Electronics Engineering*, Kyoto, Japan, August 1–3, 2010: 103–107.
- [22] LIU T J C. Finite element modeling of melting crack tip under thermo-electric Joule heating[J]. *Engineering Fracture Mechanics*, 2011, 78: 666–684.
- [23] CAI G X, YUAN F G. Stresses around the crack tip due to electric current and self-induced magnetic field[J]. *Advances in Engineering Software*, 1998, 29: 297–306.
- [24] CAI G X, YUAN F G. Electric current-induced stresses at the crack tip in conductors[J]. *International Journal of Fracture*, 1999, 96: 279–301.
- [25] CHENG D K. *Field and wave electromagnetics*[M]. MA: Addison-Wesley, 1983.
- [26] INCROPERA F P, DEWITT D P. *Fundamentals of heat and mass transfer*[M]. 5th edition. New York: John Wiley & Sons, Inc., 2002.
- [27] BORESI A P, CHONG K P. *Elasticity in engineering mechanics*[M]. 2th ed. New York: John Wiley & Sons, Inc., 2000.
- [28] ANSYS 10.0: online documentation[DB / OL]. Canonsburg, PA: ANSYS Inc, 2005. <http://www.ansys.com/Support/Documentation/>.
- [29] SOSNIN O V, GROMOVA A V, FLVANOY Y, et al. Control of austenite steel fatigue strength[J]. *International Journal of Fatigue*, 2005, 27: 1186–1191.
- [30] QIN Rongshan, SU Shengxia. Thermodynamics of crack healing under electropulsing[J]. *Journal of Materials Research*, 2002, 17(8): 2048–2052.
- [31] MA Bingdong, ZHAO Yuguang, BAI Hui, et al. Gradient distribution of mechanical properties in the high carbon steel induced by the detour effect of the pulse current[J]. *Materials and Design*, 2013, 49: 168–172.
- [32] NISHIMURA Toshihiko. Experimental and numerical evaluation of crack arresting capability due to a dimple[J]. *Transactions of the ASME*, 2005, 127: 244–250.

### Biographical notes

YU Jing, born in 1984, is currently a PHD candidate at *Institute of Sustainable Design and Manufacture, Dalian University of Technology, China*. Her research interests include remanufacturing technology, crack arrest technology, etc.  
Tel: +86-13804960235; E-mail: yj.0730.kb@163.com

ZHANG Hongchao, born in 1953, is currently a professor and a doctoral supervisor at *Dalian University of Technology, China*. His main research interests are sustainable design and manufacturing, life cycle assessment, green manufacturing, remanufacturing.  
E-mail: hongchao18@163.com

DENG Dewei, born in 1974, is currently an associate professor at *Dalian University of Technology, China*. He received his PhD degree from *Dalian University of Technology, China*, in 2003. His main research interests are surface material microscopic structure analysis and test, nuclear pump material research and application, sustainable manufacturing and remanufacturing.  
E-mail: deng@dlut.edu.cn

HAO Shegnzhi, born in 1970, is currently an associate professor at *Dalian University of Technology, China*. He received his PhD degree from *Dalian University of Technology, China*, in 2000. His main research interest is surface treatment by high current pulsed electron beam.  
E-mail: ebeam@dlut.edu.cn

IQBAL Asif, born in 1975, is currently an associate professor at *Dalian University of Technology, China*. He received his PhD degree from *Nanjing University of Aeronautics and Astronautics, China*, in 2006. His main research interests are high-speed milling, intelligent manufacturing, energy modeling of machining processes for sustainability.  
E-mail: asif.asifiqbal@gmail.com